Oleuropein Inhibits Invasion of Squamous Cell Carcinoma of the Head and Neck Through TGF-β1 Signaling Pathway

Ting Xu (tingband1983@163.com)
Wuxi Second Clinical Medical College of Nantong University
Xuan Liu
Wuxi Second Clinical Medical College of Nantong University

Research Article

Keywords: Oleuropein, SCCHN, Epithelial-mesenchymal transition, TGF-β1, Metastasis

Posted Date: February 24th, 2022

DOI: https://doi.org/10.21203/rs.3.rs-1301794/v1

Abstract

We first examined the effects of oleuropein (OL) on TGF-β1-mediated signal pathway in Tu686 tumor cells. Through morphological and Western blotting assays, we found that OL reversed the TGF-β1-induced EMT, and changed the morphology of cells and the expression levels of epithelial and interstitial markers. Wound-healing and transwell invasion assay indicated that OL reversed the TGF-β1-promoted cell migration and invasion dramatically. The effects of OL were further verified in xenograft tumor model. Due to the low toxicity and less side effects, OL may be of potential value in the inhibition of metastasis of SCCHN and improve survival.

Introduction

Squamous cell carcinoma of the head and neck (SCCHN) is the sixth most common cancer worldwide (1). Appropriately, 550, 000 cases were newly diagnosed each year, and 300, 000 deaths were linked to SCCHN. Metastasis is a leading cause to the poor prognosis of the disease (2). The underlying mechanisms of metastasis is a complicated process, but epithelial-mesenchymal transition (EMT) was deemed to be one of the main pathways leading to tumor invasion and metastasis (3). EMT is a biological process with regard to cell transformation from epithelial state to interstitial state and acquisition of migration and invasion. Previous studies showed that EMT was associated with self-renewal traits, and the promotion of tumor initiation, apoptosis and therapeutic resistance (4). Moreover, EMT is related to the activation of Smad2/3-dependent signaling pathway mediated by TGF-β1 (5).

TGF-β1 is a key regulator of cell proliferation and differentiation, and belongs to the differentiation β superfamily cytokines. It can not only activate the phenotype transformation of normal fibroblasts, but also stimulates mesenchymal original cells (6). Furthermore, TGF-β1-induced EMT is mainly mediated by either Smad-dependent or Smad-independent pathways. It was reported that TGF-β1 induced the EMT process by activating Smad2 signal in SCCHN cell line Tu686 (7). Thus, the activation of anti-EMT pathway, or the inhibition of TGF-β1 signaling, was considered to provide a potentially novel target for the treatment of SCCHN.

Oleuropein (OL), a natural antioxidant molecule extracted from olive leaves, has been reported to be associated with the beneficial effects of the plant on human (8–10). Studies revealed that OL can suppress the EMT alterations of peritoneal cells during peritoneal dialysis, so as to alleviate the toxicity reaction of dialysis (11). In addition, it was reported that OL inhibits the migration through suppression of EMT in breast cancer cells (12), and it also inhibits the proliferation of colorectal cancer cell through downregulation of HIF-1α signal (13). HIF-1α-regulated TGF-β1 can induce EMT to promote the progression of breast cancer (14), and induction of EMT via Wnt/β-catenin signaling has been shown to be driven by HIF-1α in prostate and hepatocellular carcinoma (15, 16). In this study, we demonstrated that OL inhibits the growth and metastasis of SCCHN by interfering with the TGF-β1 signaling pathway. These results will play a guiding role in the prevention and treatment of SCCHN.

Materials And Methods

Cell culture and treatment. Human squamous cell carcinoma of head and neck cell line Tu686 and its corresponding high metastasis potential cell line M2 (Shanghai NuoChen Biotechnology Co., Ltd) were cultured in 10% fetal bovine serum (FBS) and Dulbecco's Modified Eagle Medium (DMEM) F12 medium (Gibco, Grand Island, NY, USA), 100 IU/ml penicillin and 100 IU/ml streptomycin at 37 ˚C in a humidified atmosphere with 5% CO_2. The appropriate treatment concentration of TGF-β1 (Recombinant human TGF-β1, Peprotech, USA) was 10 ng/ml according to previous study (7). OL (CAS no. 10596-60-1, molecular weight 540.514, Shanghai Yeyuan Biology) powder, was resuspended by precooled sterile PBS, with a final concentration of 1 mg/ml (stored at -20 ˚C), and diluted with PBS and the appropriate concentration was selected by cell viability assay. The morphological changes of cells were observed under an inverted fluorescence microscope (Leica DMI3000B, German).

MTT assay. Cell viability was detected with the 3-(4,5-dimethyl-thiazol-2-yl)-2,5 diphenyltetrazolium (MTT) assay. Tu686 cells (1×10^4 cells per well) were cultured in 96-well plates. The cells were adhered to the wall on the next day and were starved in serum-free medium overnight. Then the cells were exposed to preset concentrations of OL. After another 24 h, 150 μl of MTT (2 μg/ml; Sigma-Aldrich) was added for incubation at 37 ˚C. Formazan crystals were dissolved in DMSO and the absorbance was measured at 570 nm using a Beckman Coulter microplate reader.

Apoptosis assay. Cells were inoculated into six-well plates in a density of 1×10^5 cells/well. The next day, the medium was replaced after 5 h of TGF-β1 (10 ng/ml) and/or OL (25 μg/ml) treatment. After another 24 h, the cells were collected, centrifuged at 200 g and resuspended. Cells were then stained by Annexin V-FITC according to the protocol of Annexin V-PI apoptosis detection kit (Kaiji Biology, Jiangsu). Twenty min later, propid iumiodide (PI) was added for another 5 min. Then the cells were analyzed by flow cytometry.

Scratch and invasion assay. Tu686 cells were seeded onto each well of the six-well plates (2×10^5 cells per well) and allowed to grow to 90% confluence, then they were placed into serum-free medium for 24 h. The cells were scratched with a 200-μl pipette tip and the non-adherent cells were washed off with medium. Cells were then treated with PBS, TGF-β1 (10 ng/ml) and TGF-β1 (10 ng/ml) + OL (25 μg/ml). Migration of wounded cells was observed and photographed at 0 and 24 h with a microscope previously described. Three different areas in each assay were chosen to measure the distance of migrating cells. For invasion assay, 3×10^4 Tu686 cells in 100 μl of serum-free medium, treated with 10 ng/ml TGF-β1, or with 10 ng/ml TGF-βl + 25 μg/ml OL, were seeded in the upper chamber of Matrigel coated inserts (8 μm pores; BD Bioscience). Following incubation for 24 h, the cells which penetrated the filters were stained with gentian violet. The number of invasive cells was determined by counting all cells attached to the bottom of the inserts under an inverted microscope at ×100 magnification. Both assays were carried out in triplicate.

Western blotting. The assay was performed as previously described (17). Briefly, a total of 50 μg proteins were extracted from the cells or tissues of each group. After electrophoresis, transmembrane and

blocking, the blotted membranes were incubated with anti-E-cadherin (ab40772, abcam, 1:500), anti-Vimentin (ab92547, abcam, 1:500), anti-Snail (ab216347, abcam, 1:1,000), anti-Smad2 (ab280888, abcam, 1:1000), anti-p-Smad2 (3140, Cell Signaling, 1:500), anti-Smad4 (ab40759, abcam, 1:1000), anti-MMP9 (3852, Cell Signaling, 1:1000), anti-N-Cadherin (ab76011, abcam, 1:1000), anti-HIF-1α (ab1, abcam, 1:1000), anti-AKT (9271, Cell Signaling, 1:500), anti-p-AKT (9271, Cell Signaling, 1:500), anti-PHD2 (3293, Cell Signaling, 1:1000) antibodies at 4 ˚C overnight. Subsequent to being washed, the membranes were incubated with HRP-labeled secondery antibodies (Boster Biological Engineering, Wuhan) for 1 h at room temperature. Bands were visualized by employing the BeyoECL Plus Detection system (Beyotime Institute of Biotechnology, Jiangsu, China). The intensity of protein fragments was quantified with Quantity One software (4.5.0 Basic; Bio-Rad, Hercules, CA, USA) and represented as the densitometric ratio of the targeted proteins to β-actin. All cell protein lysates were assayed in triplicate.

Xenograft tumor experiments. Male, 5 to 7-week-old BALB/c nude mice were purchased from Changzhou Cavens Animal Experiment Company and raised in SPF animal experiment center. Ten mice were divided into control and OL treatment groups. Preparation of cells for transplantation injection: the M2 cells for control group and OL group were treated with PBS and 1200 μg/ml of OL, respectively, after incubation for 24 h, the cells were collected. On the day of inoculation, tumor cells at 70%-80% confluence were trypsinized and resuspended in FBS-free culture medium. A volume of 100 μl single cell suspension was injected into the subcutaneous area of mice, and whether there were colliculus and redness in the injection area was observed. After inoculation, they were kept in SPF animal room. The lengths and widths of the tumors were measured with vernier calipers, and tumor volumes were calculated using the following formula: tumor volume = length × width^2 × 0.5. Two weeks later, the mice were sacrificed and the tissues were obtained for Western blotting assay. The use of animals in the present study was complied with the Guide for the Care and Use of Laboratory Animals. This study was approved by the Ethics Committee of Wuxi Second People's Hospital. The approval number is (2021) ethical review NO. (Y-13). All methods were reported in accordance with the ARRIVE guidelines. The tissue sections were viewed at ×100 magnification, and images were captured with a digital camera.

Statistical analysis. The statistical analysis software package (SPSS 11.5, Inc., Chicago, IL, USA) was employed for data analysis. The Student's t-test and Mann-Whitney U test were used for the statistical analysis of data. Difference at $P < 0.05$ was considered to indicate a statistical significance.

Results

Selection of suitable dose of OL by MTT. The intervention concentration of OL was set to 0, 2.5, 5, 10, 25, 50, 75, 100, 125, 150, and 200 μg/ml, respectively. By analyzing the cell proliferation activity, we found that it had no side effects on the Tu686 cells under the concentration of 25 μg/ml (see Fig. 1A).

OL promotes apoptosis of Tu686 cells. The number of Q2 + Q3 cells was obtained from Apoptosis FACS data and utilized for the evaluation of cell apoptosis. After TGF-β1 intervention, the number of apoptotic cells decreased slightly without statistically significant difference compared with the control group. After

adding both TGF-β1 and OL for intervention, the apoptosis rate of Tu686 cells increased significantly when compared with that of the TGF-β1 alone group ($P < 0.05$) (Fig. 1B, C).

OL reverses TGF-β1-induced EMT of Tu686 cells. It was observed under the microscope that after the addition of 10 ng/ml of TGF-β1, the Tu686 cells showed obvious changes of EMT. That is, the connection between the epithelium was loose and the antennae were extended, showing changes similar to EMT. Nevertheless, after the addition of 25 μg/ml of OL, the antennae of stromal like cells became shorter and the cell arrangement was closer than that of the cells treated with TGF-β1 alone, which showed changes similar to mesenchymal epithelial transformation (MET) (Fig. 2A).

OL attenuates the enhanced migration and invasion of Tu686 cells induced by TGF-β1. Stimulation with a dose of 10 ng/ml of TGF-β1 could greatly enhance the migration and invasion ability of Tu686 cells. However, after adding OL (25 μg/ml) for treatment for 24 h, it was observed that the enhancement of migration and invasion induced by TGF-β1 was significantly inhibited. (Fig. 2B-E).

OL affects the expression of EMT-related proteins. After treatment with TGF-β1, the expression level of E-cadherin was significantly downregulated, and the levels of Vimentin, Snail and MMP9 were significantly increased. After the treatment with both TGF-β1 and OL, the decreased level of E-cadherin was significantly reversed, while the expression levels of snail and MMP9 were significantly decreased compared with the TGF-β1 alone group (Fig. 3).

OL affects the classical TGF-β1-Smad2 signaling pathway. The phosphorylation level of Smad2 was significantly increased after the intervention of TGF-β1 (10 ng/ml), while this increase was significantly inhibited by the treatment of OL (25 μg/ml) (Fig. 4A).

OL affects HIF-1α-related signaling pathways induced by TGF-β1. After adding OL (25 μg/ml), the increased level of HIF-1α induced by TGF-β1 (10 ng/ml) was significantly attenuated (Fig. 4B). The phosphorylation level of AKT was significantly increased after the intervention of TGF-β1, while it was significantly inhibited after the addition of OL. The expression level of PDH2 significantly decreased after the treatment with TGF-β1, while OL treatment partly reversed it (Fig. 4C).

OL inhibits the growth of SCCHN in vivo. The xenograft tumor-bearing mice injected with M2 cells, which were treated with PBS or OL (1200 μg/ml), were used for tumor observation for 14 days post-transplantation. We found that the volume of xenograft tumors in the OL treatment group was significantly smaller when compared with that of the control group (Fig. 5A, B).

OL alters the expression of EMT and metastasis-associated proteins in xenograft tumor tissues. The expression levels of E-cadherin and PHD2 were significantly increased in the xenograft tumor tissues from mice injected with M2 cells treated with OL, when compared with the results from the control group. The expression levels of N-cadherin, Vimentin, Snail, MMP9 and HIF-1α were significantly decreased in the xenograft tumor tissues from mice injected with M2 cells treated with OL, when compared with the control group (Fig. 6A-H).

Discussion

Previous studies have shown that OL demonstrated anti-cancer effects in various types of tumors (18). The prognosis is commonly poor when metastasis occurred in SCCHN patients. For those elder or advanced patients with metastasis, who have missed appropriate opportunity for surgery, radiotherapy and chemotherapy are deemed to be the most optimal treatment approach. Therefore, it is of particular importance to develop novel agents with favorable anticancer effect and tolerable toxicity and side effects. As a natural compound, OL shows low toxicity to human body, thus the prognosis of patients may be significantly improved when it could be applied for adjuvant chemotherapy in the future. However, the effect of OL on SCCHN has not been reported yet. In this study, a suitable non-toxic dose range of OL was screened through MTT test. The results were similar to the peritoneal dialysis test conducted by Lupinaccis *et al*. (11). After the addition of 25 μg/ml of OL, the apoptosis rate of Tu686 cells was significantly increased, which indicated that OL may effectively induce apoptosis of SCCHN cells *in vitro*, and this finding is consistent with the antitumor effect of OL in other tumors.

Inhibition of metastasis is considered to be in the top priority to improve the prognosis of SCCHN. TGF-β1 can induce EMT alterations in Tu686 cells and promote cell invasion *in vitro* (7). When OL intervention was added in this study, we observed that the change of morphology of Tu686 cells was reversed, with morphological changes similar to MET. Morphologically, cells in TGF-β1 + OL group were similar to that of the control group, and this finding was consistent with the study of Lupinaccis *et al*. This indicates that the effect of OL on reversing EMT is stable either in the process of promoting fibrosis or tumor metastasis. Scratch and Transwell assays verified that OL could reverse TGF-β1-induced migration and invasion of Tu686 cells. When the EMT process is activated, the expression of epithelial cell marker protein E-cadherin decreases, whereas the expression of interstitial cell marker proteins such as N-cadherin and Vimentin increases (19). Many transcription factors, especially the Snail family, mediate the process of EMT. MMP9, one of the matrix metalloproteinases and most commonly involved in the EMT of SCCHN, can promote tumor invasion and metastasis by degrading extracellular matrix (ECM). At present, several studies were conducted about the inhibitory effects on tumor invasion and metastasis of OL or its related compounds in breast cancer, colon cancer and melanoma (12, 20, 21). Among them, OL inhibits invasion by regulating EMT in MCF-7 cells of breast cancer. Our study showed that when OL was added, TGF-β1-induced changes of E-cadherin, Vimentin, Snail and MMP-9 were partially reversed, which further confirmed that OL could inhibit the invasion and migration of Tu686 cells *in vitro*.

We further detected the classical signal pathway involved in TGF-β1-induced EMT, Smad2/3 signal pathway. The phosphorylation level of Smad2 decreased significantly in TGF-β1 + OL group when compared with that of the TGF-β1 group. A previous study showed that OL inhibits the proliferation of colorectal cancer cells through downregulation of HIF-1α (13). Our previous study also revealed that HIF-1α played an important regulatory role in OL-enhanced radiosensitivity of nasopharyngeal carcinoma (22). HIF-1α, the principal regulator of hypoxia, mediates a variety of biological processes in tumor cells, including EMT (23). In this study, TGF-β1 significantly increased HIF-1α expression in Tu686 cells, whereas the HIF-1α level was decreased by OL. There are multiple signaling pathways involved in HIF-1α

regulation, including oxygen-dependent and oxygen-independent pathways. In this study, we detected the activation levels of PHD2 and AKT/pAKT which are involved in pVHL-dependent pathway and growth factor signaling pathway, respectively. The results showed that TGF-β1 significantly decreased PHD2 expression and OL partially reversed it. As we know, PHDs is an upstream regulator of HIF-1α, and its expression can be downregulated by hypoxia and consequently the degradation of HIF-1α is reduced (24). In this study, TGF-β1 intervention alone rather than hypoxic environment can also affect the expression of PHD2, and this result was similar to a study reported in 2013, which suggests that TGF-β1 decreases PHD2 expression via a Smad-dependent signaling pathway, thereby leading to HIF-1α accumulation and EMT in renal tubular cells (25). Those demonstrated that PHDs can act through oxygen-independent pathway. Meanwhile, OL is able to reverse TGF-β1/PHD2/HIF-1α signaling pathway. PI_3K/AKT signal is involved in the growth factor signaling pathways. We found that TGF-β1 significantly increased the phosphorylation of AKT, which was effectively inhibited by OL. These findings suggest that OL can regulate the process of EMT by regulating the expression of HIF-1α. There are some complicated cross-talks between TGF-β1 signal, HIF-1α signal and PI_3K/AKT signal, which need further investigation. The schematic diagram of OL intervention in TGF-β1 signaling pathway is shown in Fig. 7.

In order to further clarify the effect of OL on SCCHN, subcutaneous xenograft model of SCCHN cancer cells in nude mice was established. Advanced metastatic SCCHN cell line M2 was applied in this study. The tumor volume in OL group (mice injected with cells pretreated with OL) was smaller than that of the control group, indicating that OL has significant antitumor effect *in vivo*. In the verification of metastatic capacity of tumor cells, proteins in tumor tissues were extracted to detect the expression of EMT-related proteins. OL can significantly enhance the expression of epithelial cell marker E-cadherin, and reduce the expression of interstitial cell markers Vimentin, N-cadherin, and EMT-related transcription factor snail, indicating that OL effectively intervened the process of EMT *in vivo*. The change of MMP9 suggests that OL could inhibit the invasion and metastasis of SCCHN tumor cells. In addition, we also detected the levels of HIF-1α and PHD2 in tissues of these two groups. OL significantly decreased the level of HIF-1α, but increased the expression of PHD2, showing the expression level of HIF-1α was negatively correlated with PHD2. These findings show that HIF-1α signaling may be involved in the inhibitory effect of OL on tumor metastasis *in vivo*.

In conclusion, this study preliminarily clarified that OL can inhibit the process of EMT, invasion and metastasis of SCCHN *in vitro* and *in vivo*. The findings of this study provide a basis for the application of this natural compound in the treatment of SCCHN in the future. The comprehensive mechanisms involved need to be further investigated.

Declarations

Acknowledgements

Not applicable.

Funding

This study was supported by Wuxi Double Hundred Top Talent Project (No. BJ2020038).

Availability of data and materials

All data generated or analyzed during this study are included in this published article.

Authors' contributions

TX contributed to the study concept, design, data statistics and most manual writing, TX and XL participated in the writing of some manual works.

Ethics approval and consent to participate

The study was approved by the Ethics Committee of Wuxi Second People's Hospital. The approval number is: (2021) ethical review NO. (Y-13). All methods were carried out in accordance with relevant guidelines and regulations. No human being was involved in this study thus informed consent was not in need.

Patient consent for publication

Not applicable.

Competing interests

The authors declare that they have no competing interests.

References

1. Fitzmaurice C, Allen C, Barber RM, Barregard L, Bhutta ZA, Brenner H, et al. Global, Regional, and National Cancer Incidence, Mortality, Years of Life Lost, Years Lived With Disability, and Disability-Adjusted Life-years for 32 Cancer Groups, 1990 to 2015: A Systematic Analysis for the Global Burden of Disease Study. *JAMA oncology* (2017) 3(4):524-48. Epub 2016/12/06. doi: 10.1001/jamaoncol.2016.5688. PubMed PMID: 27918777; PubMed Central PMCID: PMCPMC6103527.
2. Jin Z, Zhao X, Cui L, Xu X, Zhao Y, Younai F, et al. UBE2C promotes the progression of head and neck squamous cell carcinoma. *Biochemical and biophysical research communications* (2020) 523(2):389-97. Epub 2019/12/25. doi: 10.1016/j.bbrc.2019.12.064. PubMed PMID: 31870550.
3. Thiery JP. EMT: An Update. *Methods in molecular biology (Clifton, NJ)* (2021) 2179:35-9. Epub 2020/09/18. doi: 10.1007/978-1-0716-0779-4_6. PubMed PMID: 32939712.
4. Zhang Y, Weinberg RA. Epithelial-to-mesenchymal transition in cancer: complexity and opportunities. *Frontiers of medicine* (2018) 12(4):361-73. Epub 2018/07/26. doi: 10.1007/s11684-018-0656-6.

PubMed PMID: 30043221; PubMed Central PMCID: PMCPMC6186394.

5. Mittal V. Epithelial Mesenchymal Transition in Tumor Metastasis. *Annual review of pathology* (2018) 13:395-412. Epub 2018/02/08. doi: 10.1146/annurev-pathol-020117-043854. PubMed PMID: 29414248.
6. Wu YL, Zhang YJ, Yao YL, Li ZM, Han X, Lian LH, et al. Cucurbitacin E ameliorates hepatic fibrosis in vivo and in vitro through activation of AMPK and blocking mTOR-dependent signaling pathway. *Toxicology letters* (2016) 258:147-58. Epub 2016/07/02. doi: 10.1016/j.toxlet.2016.06.2102. PubMed PMID: 27363783.
7. Yu C, Liu Y, Huang D, Dai Y, Cai G, Sun J, et al. TGF-β1 mediates epithelial to mesenchymal transition via the TGF-β/Smad pathway in squamous cell carcinoma of the head and neck. *Oncology reports* (2011) 25(6):1581-7. Epub 2011/04/12. doi: 10.3892/or.2011.1251. PubMed PMID: 21479366.
8. Lu HY, Zhu JS, Xie J, Zhang Z, Zhu J, Jiang S, et al. Hydroxytyrosol and Oleuropein Inhibit Migration and Invasion via Induction of Autophagy in ER-Positive Breast Cancer Cell Lines (MCF7 and T47D). *Nutrition and cancer* (2021) 73(2):350-60. Epub 2020/04/15. doi: 10.1080/01635581.2020.1750661. PubMed PMID: 32286090.
9. Goldsmith CD, Bond DR, Jankowski H, Weidenhofer J, Stathopoulos CE, Roach PD, et al. The Olive Biophenols Oleuropein and Hydroxytyrosol Selectively Reduce Proliferation, Influence the Cell Cycle, and Induce Apoptosis in Pancreatic Cancer Cells. *International journal of molecular sciences* (2018) 19(7). Epub 2018/07/14. doi: 10.3390/ijms19071937. PubMed PMID: 30004416; PubMed Central PMCID: PMCPMC6073890.
10. Zhang F, Zhang M. Oleuropein inhibits esophageal cancer through hypoxic suppression of BTG3 mRNA. *Food & function* (2019) 10(2):978-85. Epub 2019/02/01. doi: 10.1039/c8fo02223b. PubMed PMID: 30702111.
11. Lupinacci S, Perri A, Toteda G, Vizza D, Puoci F, Parisi OI, et al. Olive leaf extract counteracts epithelial to mesenchymal transition process induced by peritoneal dialysis, through the inhibition of TGFβ1 signaling. *Cell biology and toxicology* (2019) 35(2):95-109. Epub 2018/07/07. doi: 10.1007/s10565-018-9438-9. PubMed PMID: 29978330.
12. Choupani J, Alivand MR, S MD, Zaeifizadeh M, M SK. Oleuropein inhibits migration ability through suppression of epithelial-mesenchymal transition and synergistically enhances doxorubicin-mediated apoptosis in MCF-7 cells. *Journal of cellular physiology* (2019) 234(6):9093-104. Epub 2018/10/15. doi: 10.1002/jcp.27586. PubMed PMID: 30317622.
13. Cárdeno A, Sánchez-Hidalgo M, Rosillo MA, Alarcón de la Lastra C. Oleuropein, a secoiridoid derived from olive tree, inhibits the proliferation of human colorectal cancer cell through downregulation of HIF-1α. *Nutrition and cancer* (2013) 65(1):147-56. Epub 2013/02/02. doi: 10.1080/01635581.2013.741758. PubMed PMID: 23368925.
14. Peng J, Wang X, Ran L, Song J, Luo R, Wang Y. Hypoxia-Inducible Factor 1α Regulates the Transforming Growth Factor β1/SMAD Family Member 3 Pathway to Promote Breast Cancer

Progression. *Journal of breast cancer* (2018) 21(3):259-66. Epub 2018/10/03. doi: 10.4048/jbc.2018.21.e42. PubMed PMID: 30275854; PubMed Central PMCID: PMCPMC6158164.

15. Jiang YG, Luo Y, He DL, Li X, Zhang LL, Peng T, et al. Role of Wnt/beta-catenin signaling pathway in epithelial-mesenchymal transition of human prostate cancer induced by hypoxia-inducible factor-1alpha. *International journal of urology : official journal of the Japanese Urological Association* (2007) 14(11):1034-9. Epub 2007/10/25. doi: 10.1111/j.1442-2042.2007.01866.x. PubMed PMID: 17956532.
16. Zhang Q, Bai X, Chen W, Ma T, Hu Q, Liang C, et al. Wnt/β-catenin signaling enhances hypoxia-induced epithelial-mesenchymal transition in hepatocellular carcinoma via crosstalk with hif-1α signaling. *Carcinogenesis* (2013) 34(5):962-73. Epub 2013/01/30. doi: 10.1093/carcin/bgt027. PubMed PMID: 23358852.
17. Xu T, Fan B, Lv C, Xiao D. Slug mediates nasopharyngeal carcinoma radioresistance via downregulation of PUMA in a p53-dependent and -independent manner. *Oncology reports* (2015) 33(5):2631-8. Epub 2015/03/31. doi: 10.3892/or.2015.3877. PubMed PMID: 25812964.
18. Ahmad Farooqi A, Fayyaz S, Silva AS, Sureda A, Nabavi SF, Mocan A, et al. Oleuropein and Cancer Chemoprevention: The Link is Hot. *Molecules (Basel, Switzerland)* (2017) 22(5). Epub 2017/05/05. doi: 10.3390/molecules22050705. PubMed PMID: 28468276; PubMed Central PMCID: PMCPMC6154543.
19. Brabletz T, Kalluri R, Nieto MA, Weinberg RA. EMT in cancer. *Nature reviews Cancer* (2018) 18(2):128-34. Epub 2018/01/13. doi: 10.1038/nrc.2017.118. PubMed PMID: 29326430.
20. Song H, Lim DY, Jung JI, Cho HJ, Park SY, Kwon GT, et al. Dietary oleuropein inhibits tumor angiogenesis and lymphangiogenesis in the B16F10 melanoma allograft model: a mechanism for the suppression of high-fat diet-induced solid tumor growth and lymph node metastasis. *Oncotarget* (2017) 8(19):32027-42. Epub 2017/04/15. doi: 10.18632/oncotarget.16757. PubMed PMID: 28410190; PubMed Central PMCID: PMCPMC5458266.
21. Imran M, Nadeem M, Gilani SA, Khan S, Sajid MW, Amir RM. Antitumor Perspectives of Oleuropein and Its Metabolite Hydroxytyrosol: Recent Updates. *Journal of food science* (2018) 83(7):1781-91. Epub 2018/06/22. doi: 10.1111/1750-3841.14198. PubMed PMID: 29928786.
22. Xu T, Xiao D. Oleuropein enhances radiation sensitivity of nasopharyngeal carcinoma by downregulating PDRG1 through HIF1α-repressed microRNA-519d. *Journal of experimental & clinical cancer research : CR* (2017) 36(1):3. Epub 2017/01/07. doi: 10.1186/s13046-016-0480-2. PubMed PMID: 28057028; PubMed Central PMCID: PMCPMC5216549.
23. Tirpe AA, Gulei D, Ciortea SM, Crivii C, Berindan-Neagoe I. Hypoxia: Overview on Hypoxia-Mediated Mechanisms with a Focus on the Role of HIF Genes. *International journal of molecular sciences* (2019) 20(24). Epub 2019/12/11. doi: 10.3390/ijms20246140. PubMed PMID: 31817513; PubMed Central PMCID: PMCPMC6941045.
24. Masoud GN, Li W. HIF-1α pathway: role, regulation and intervention for cancer therapy. *Acta pharmaceutica Sinica B* (2015) 5(5):378-89. Epub 2015/11/19. doi: 10.1016/j.apsb.2015.05.007.

PubMed PMID: 26579469; PubMed Central PMCID: PMCPMC4629436.

25. Han WQ, Zhu Q, Hu J, Li PL, Zhang F, Li N. Hypoxia-inducible factor prolyl-hydroxylase-2 mediates transforming growth factor beta 1-induced epithelial-mesenchymal transition in renal tubular cells. *Biochimica et biophysica acta* (2013) 1833(6):1454-62. Epub 2013/03/08. doi: 10.1016/j.bbamcr.2013.02.029. PubMed PMID: 23466866; PubMed Central PMCID: PMCPMC3631109.

Figures

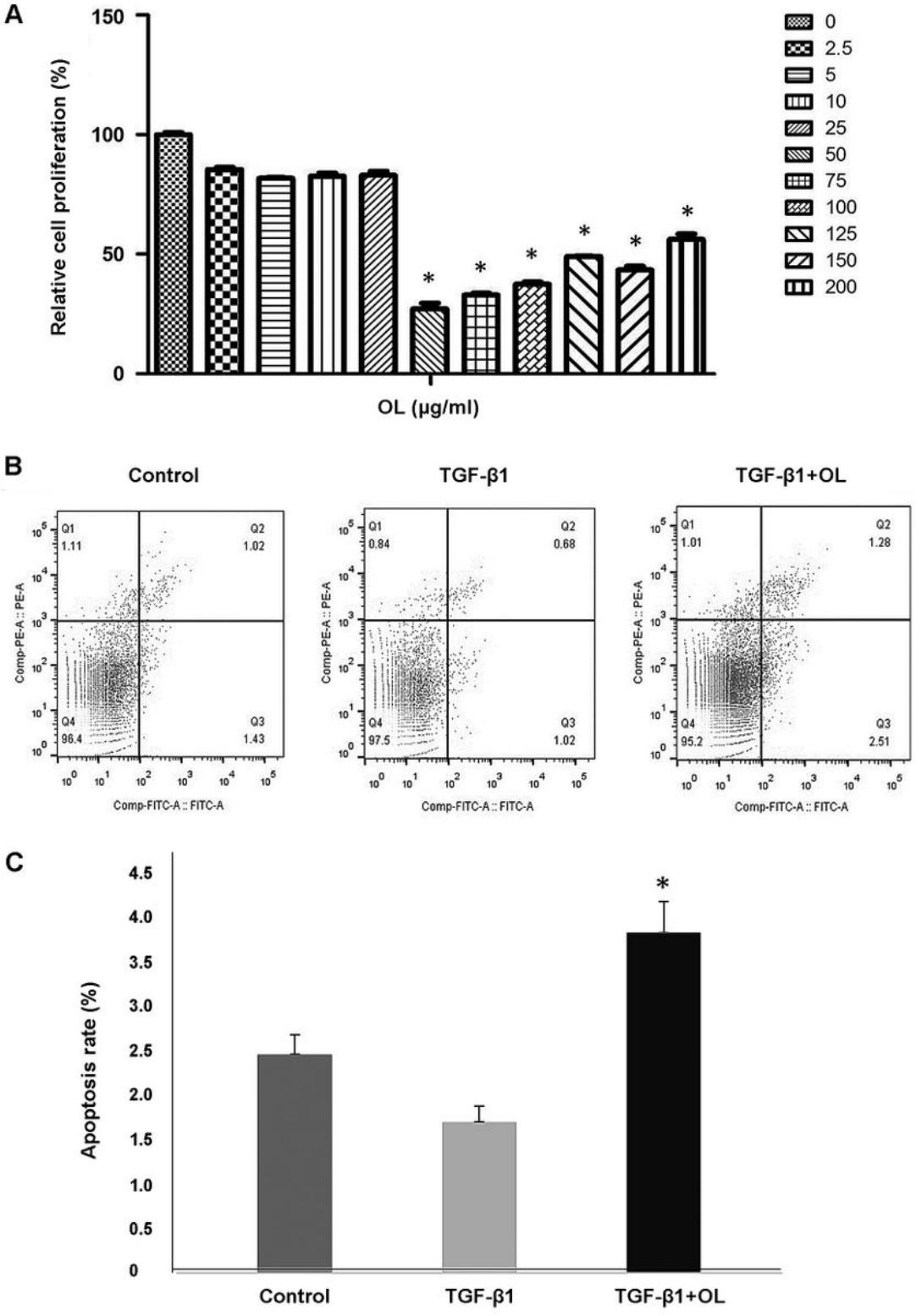

Figure 1

Effect of OL on apoptosis of Tu686 cells. (A) MTT assay was performed in Tu686 cells to determine non-toxic dose range. Cells untreated or treated with increasing doses of OL (range from 2.5-200 μg/ml) for 24 h. Cell proliferation was expressed as fold change with respect to untreated cells. *p <0.05 compared with untreated cells. (B) Flow cytometry apoptosis diagram for each group. The dose of 25 μg/ml of OL was selected for flow cytometry. The cells treated with PBS, 10 ng/ml TGF-β1, and 10 ng/ml TGF-β1 + 25

μg/ml OL were named control group, TGF-β1 group, and TGF-β1 + OL group, respectively. (C) Comparison column chart of the apoptosis rate of three groups. Total apoptosis rate (including early and late) was detected for each group. *p <0.05 vs. TGF-β1 group (tests were repeated for 3 times).

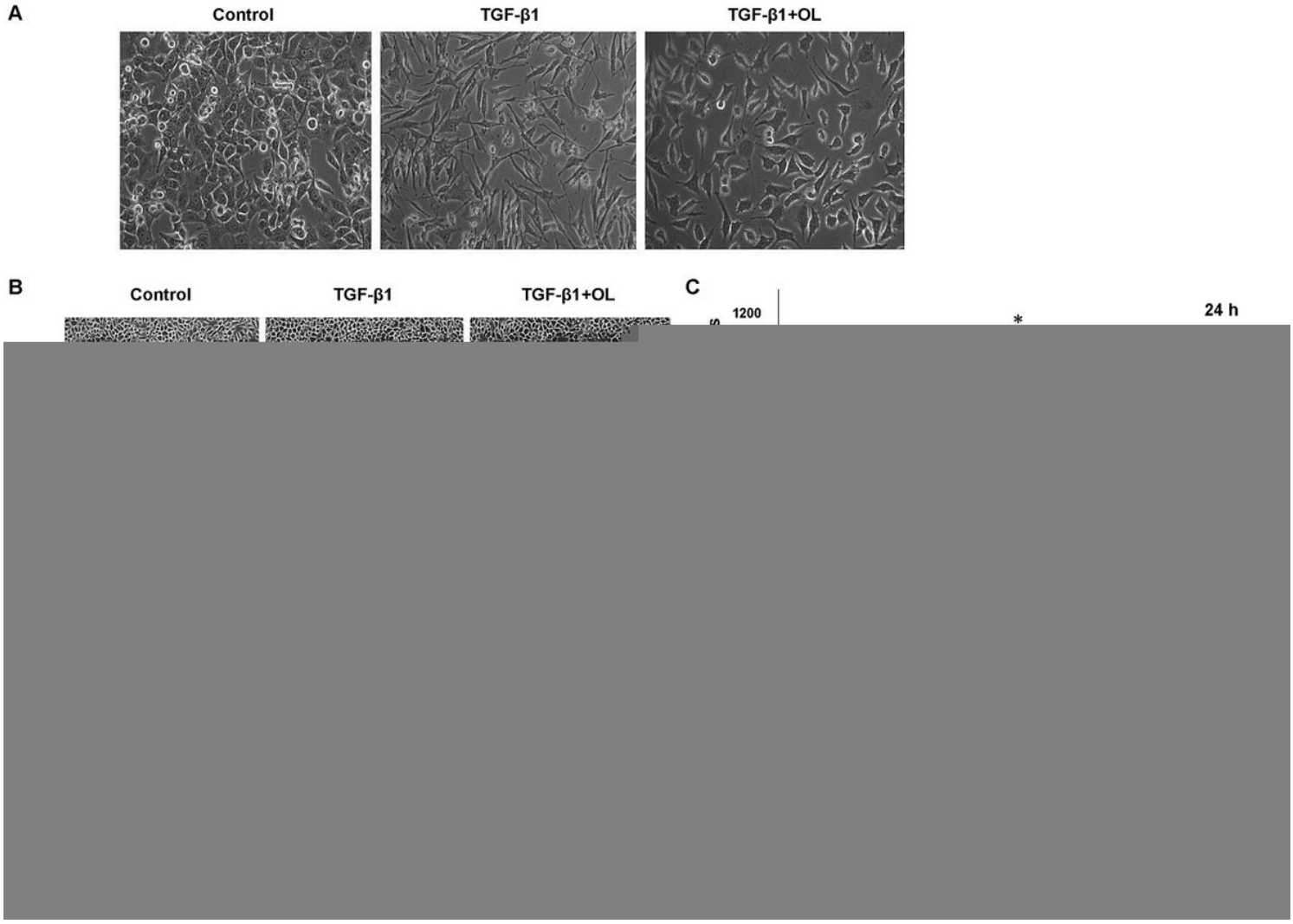

Figure 2

OL reversed EMT, migration and invasion of Tu686 cells induced by TGF-β1. (A) Morphological changes involved in OL and/or TGF-β1-treated Tu686 cells. The cells were treated with PBS, 10 ng/ml TGF-β1, and 10 ng/ml TGF-β1 + 25 μg/ml OL for 72 h. EMT changes were observed under microscope, ×100. (B) Wound-healing scratch assay photos were taken for each group (at 0 h and 24 h). (D) Transwell assay photos were taken for each group at 24 h. The column charts show the cell mobility (C) and invasive ability (E) of each group at 24 h. *p <0.05 vs. control, **p <0.05 vs. cells treated with TGF-β1 (tests were repeated for 3 times).

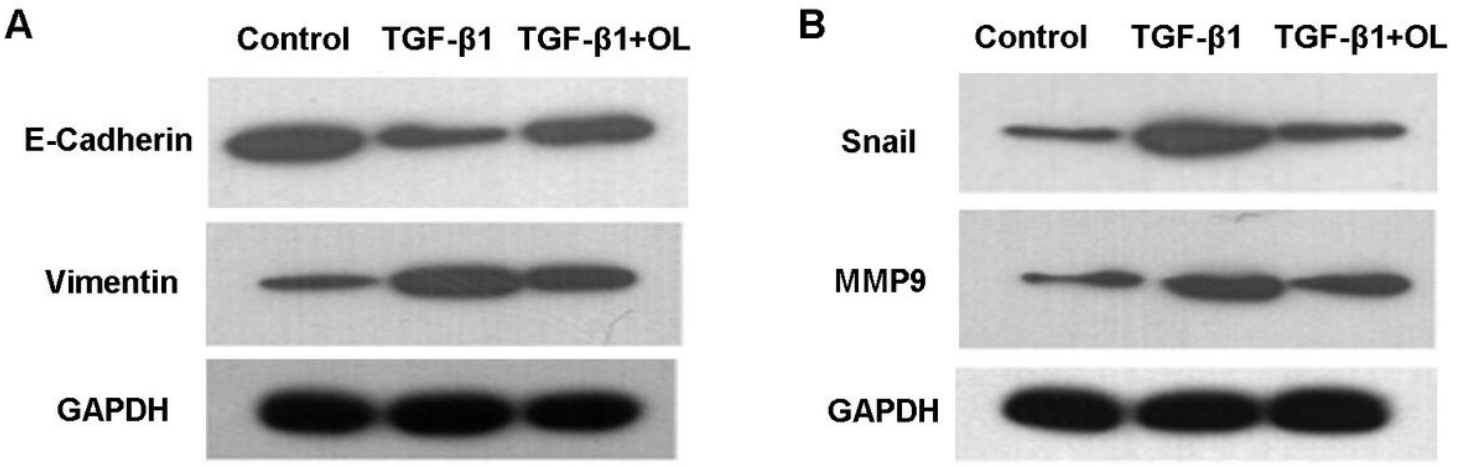

Figure 3

OL changed the expression of EMT-associated proteins in TGF-β1-treated cells. (A) Western blotting assay results about the E-cadherin and Vimentin expression in different groups (control, TGF-β1 and TGF-β1 + OL groups). (B) Western blotting results of Snail and MMP9 in different groups.

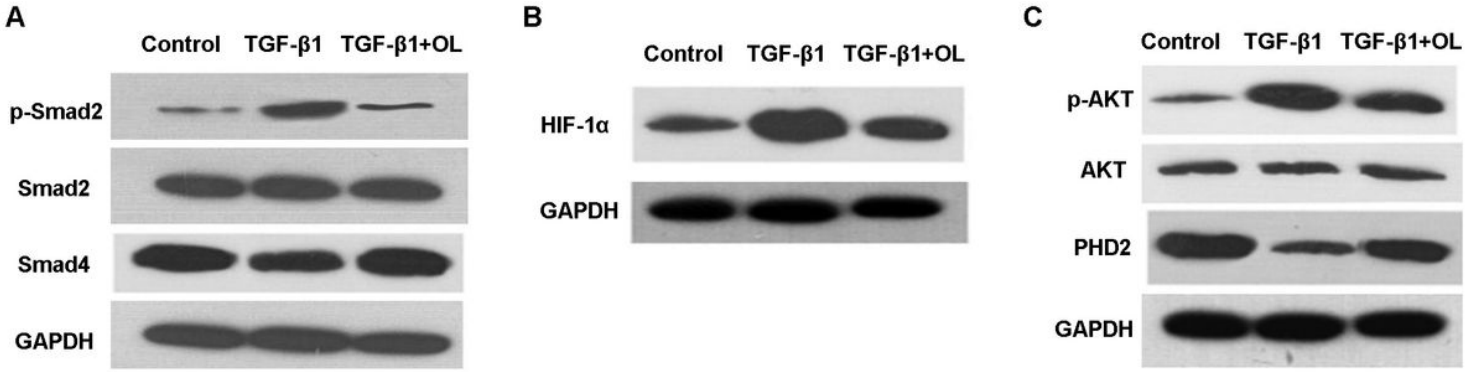

Figure 4

OL inhibited the signaling pathways involved in TGF-β1-mediated invasion and metastasis of SCCHN. Western blotting results showing that (A) TGF-β1 and OL affected the classical Smad2 signaling pathway, (B) HIF-1α expression, and (C) pVHL-dependent pathway and PI_3K/AKT signaling pathway proteins.

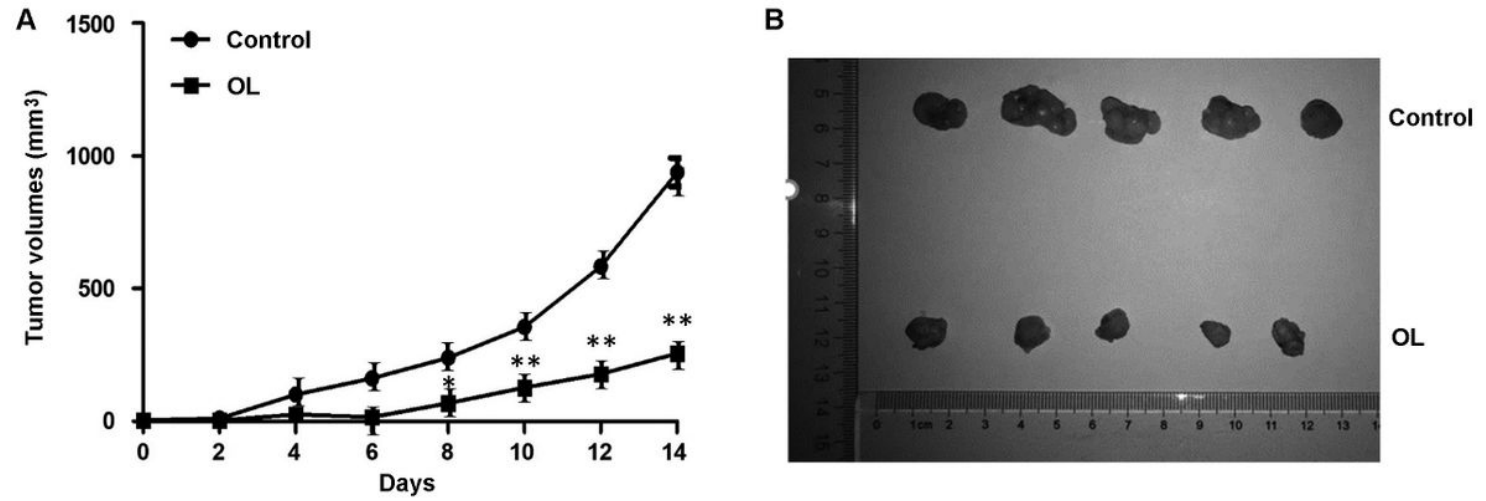

Figure 5

OL inhibits SCCHN xenograft tumor growth. M2 cells were treated with PBS (control group) and 1200 μg/ml OL (OL group) for 24 h, then the cells were subcutaneously injected into submaxillary area of 5week-old male nude mice, five mice for each group. (A) The xenograft tumor volumes were measured every two days and the growth curve was compiled (*p <0.05, **p <0.01 vs. control group). (B) The mice were sacrificed at the 14th day and the photos of xenograft tumors of the two groups were taken.

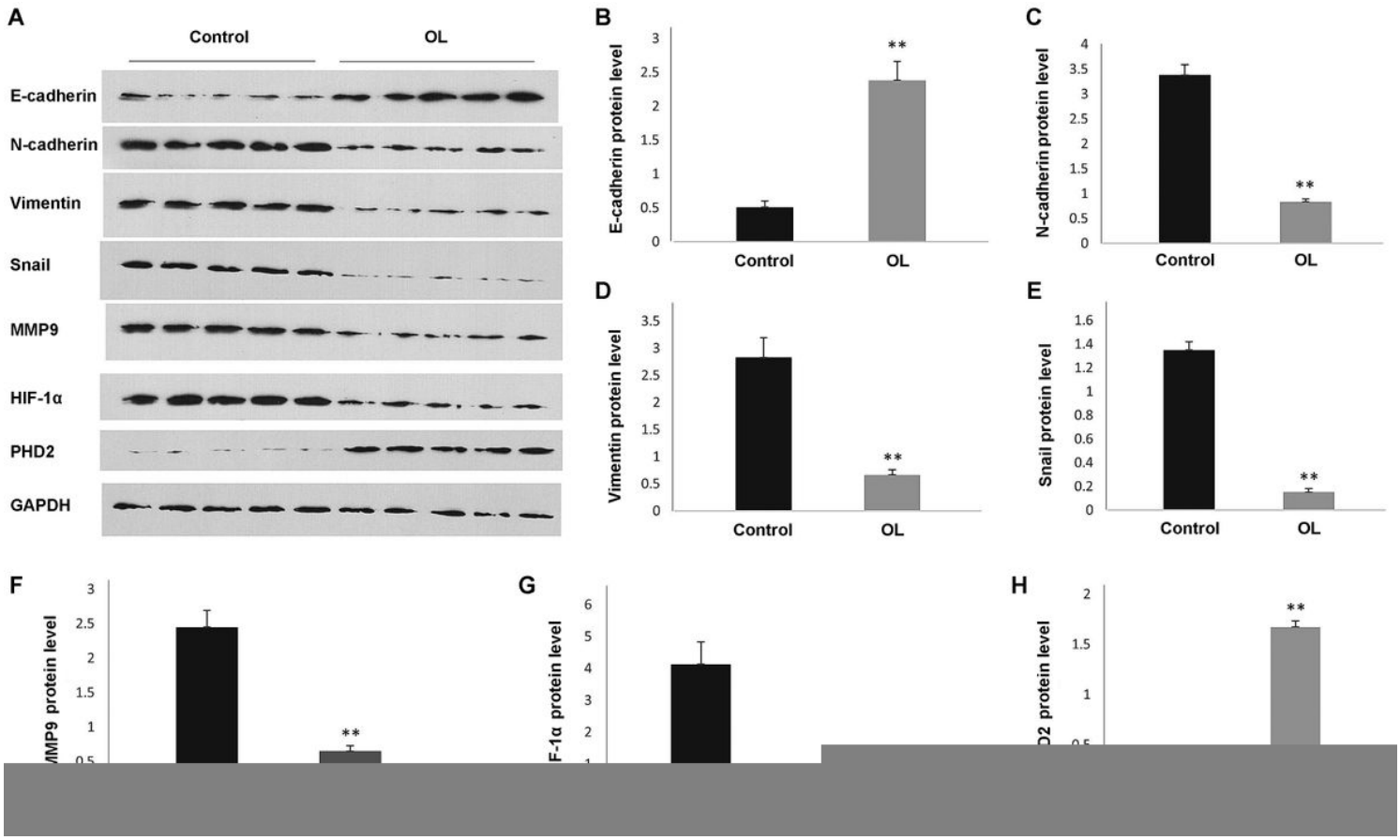

Figure 6

OL altered expression of EMT-associated proteins and some HIF-1α pathway proteins in xenograft tumor. M2 were subcutaneously injected into the submaxillary area of 5-week-old male nude mice, five mice for each group. After two weeks later, the mice were sacrificed and the tumor tissue proteins were extracted for E-cadherin, N-cadherin, Vimentin, Snail, MMP9, HIF-1α and PHD2 analysis. (A) Western blotting results of tumor tissue from 10 mice (five mice for each group) for the expression levels of target proteins. The column diagrams show the expression levels of E-cadherin (B), N-cadherin (C), Vimentin (D), Snail (E), MMP9 (F), HIF-1α (G) and PHD2 (H) between the two groups (**p <0.01 vs. control).

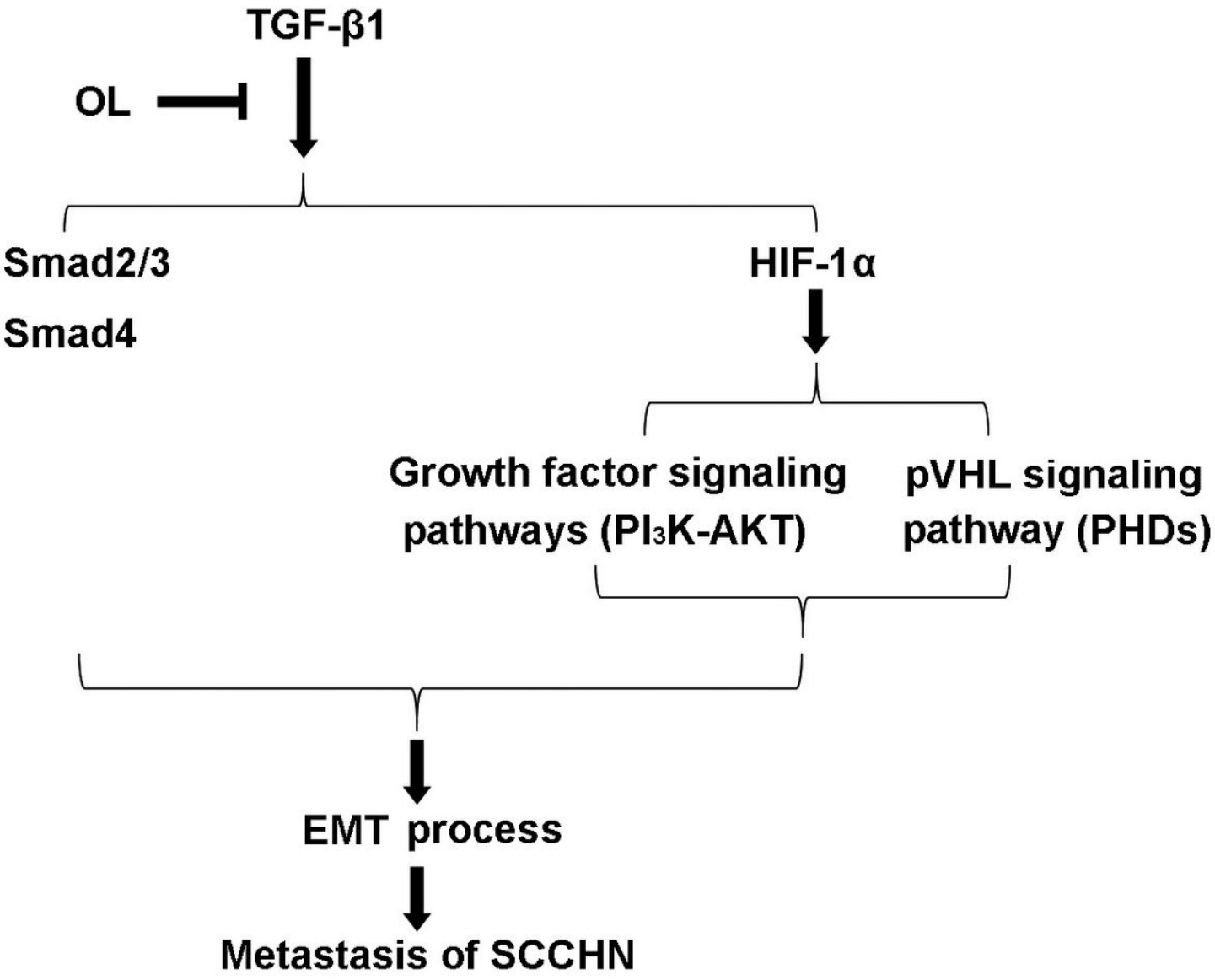

Figure 7

Schematic diagram showing the signaling pathways involved in the inhibitory effect of OL on EMT of SCCHN.